Tetrahedron 67 (2011) 9685–9689

Contents lists available at SciVerse ScienceDirect

Tetrahedron

journal homepage: www.elsevier.com/locate/tet

Gold nanoparticle-templated assembly of oligothiophenes: preparation and film properties

Ken-ichi Saitou [a], Ryuhei Nishiyabu [a], Masahiko Iyoda [b], Yuji Kubo [a,*]

[a] Department of Applied Chemistry, Graduate School of Urban Environmental Sciences, Tokyo Metropolitan University, 1-1 Minami-ohsawa, Hachioji, Tokyo 192-0397, Japan
[b] Department of Chemistry, Graduate School of Science and Engineering, Tokyo Metropolitan University, 1-1 Minami-ohsawa, Hachioji, Tokyo 192-0397, Japan

ARTICLE INFO

Article history:
Received 9 September 2011
Received in revised form 8 October 2011
Accepted 11 October 2011
Available online 20 October 2011

Keywords:
Oligothiophene
Gold nanoparticle
Self-assembly
Electric conductivity

ABSTRACT

Terthiophene-appended gold nanoparticles were prepared by the reduction of $AuCl_4^-(C_8H_{17})_4N^+$ with $NaBH_4$ in the presence of bis[2,5-di(3-hexylthiophen-2-yl)thiophene-3-carboxyloxyhexanyl]disulfide. A hexagonal self-assembly of particles with gold core diameters (1.9±0.1 nm) was detected by high-angle annular dark-field scanning transmission electron microscopy. The electric conductivity of the iodine-doped film was 9.1×10^{-6} S cm^{-1}, which was ascribable to the terthiophene-based inter-ligand π–π interactions. The Au/terthiophene hybrid spin-coated film consisted of a highly three-dimensional assembled structure of terthiophenes, as inferred from grazing-incidence small-angle X-ray scattering, indicating that such monodispersed and small-sized gold nanoparticles can serve as a template for this organization. In this study, a gold nanoparticle-templated assembly of oligothiophenes has been fabricated for proposing a method to develop tailor-made organizations of π-conjugated oligomers.

1. Introduction

π-Conjugated oligomers and polymers have attracted much attention because of their numerous applications in organic electronics,[1] such as thin-film transistors,[2] bulk-heterojunction solar cells,[3] and light-emitting materials.[4] In addition, fabrication of π-conjugated nanostructures by a supramolecular approach has generated a great deal of interest, wherein tailor-made molecular components are prepared by self-assembly.[5] In this context, conjugated oligomers are attractive because they offer advantages over the corresponding polymers in synthesis, purification, and structural definition.[6] Further, considering that electronic devices work well in solid state, controlling the supramolecular ordering is crucial for determining the characteristics, which mainly depend on the intermolecular interactions between the conjugated species and the substrate surface. However, a method for realizing the desired nanoscale organization of π-conjugated components is yet to be devised.

Gold nanoparticles are widely used as building blocks for self-assembled systems.[7] Precise control of the surface properties of nanoparticles will enable the development of hybrid materials that can be used to induce network aggregation via noncovalent supramolecular interactions.[8] Meskers et al. have developed self-organized hybrid oligo(*p*-phenylenevinylene)–gold nanoparticle tapes.[9] A remarkable feature of this structure is the proximity of the metal particles to the π-conjugated tapes, which facilitates electric communication through noncovalent interactions. We are interested in studying the manner in which a metal nanoparticle arranges self-assembled nanostructures of π-conjugated oligomers such as oligothiophenes. Although thiophene oligomers/polymer-conjugated gold nanoparticles have been widely investigated for the purpose of exploring molecular electronics,[10] the use of gold nanoparticle as templates for organization with well-defined morphologies is still in its infancy. Easy functionalization of nanoparticle surface using thiolated ligands would enable us to prepare conjugated oligothiophenes with desired self-assembled structures.

Currently, we have investigated the interplay between functional thiophenes and gold nanoparticles for integrating π-conjugated systems with inorganic nanoparticles. For instance, nanocrystallization of gold in the presence of amphiphilic polythiophenes with a cationic isothiouronium pendant has shown that the polythiophenes not only serve as a stabilizer having reduction properties for the growth process but also control the shape of the nanocrystals by tuning the reaction conditions.[11] This finding indicates that π-conjugated thiophene systems can control the characteristics of metal nanoparticles. On the other hand, there remains the subject to investigate whether metal nanoparticles with oligothiophenes bound at the surface can be used to modify the characteristics of the surface-bound oligothiophenes. Such exploration would provide a hint for preparation strategy to develop functional π-conjugated materials. In this study, we successfully

* Corresponding author. Tel./fax: +81 42 677 3134; e-mail address: yujik@tmu.ac.jp (Y. Kubo).

0040-4020/$ – see front matter © 2011 Elsevier Ltd. All rights reserved.
doi:10.1016/j.tet.2011.10.032

prepared monodispersed and terthiophene-appended gold nanoparticles having a small gold core diameter of 1.9 nm. As described in detail below, we found that the surface-bound terthiophenes were organized three-dimensionally in periodic gold particle networks. Here, the synthesis and characterization involving electric conductivity in the film are discussed.

2. Results and discussion

2.1. Synthesis

Our approach to utilize nanoparticle as a template requires not only monodispersed nanoparticles but also an alkyl spacer between an oligothiophene unit and the particle template for preventing electronic interactions between them. For the synthesis of the coating reagent we targeted bis(terthiophenecarbonyloxyhexanyl) disulfide **2**, wherein the simplest terthiophene unit was employed as an oligothiophene. Further, the disulfide could be reduced by the Brust–Schiffrin method using $NaBH_4$.[12]

The synthetic pathway is shown in Scheme 1. Suzuki–Miyaura cross-coupling reaction of methyl 2,5-dibromothiophene-3-carboxylate **3**[13] with 4 equiv of 5,5-dimethyl-2-(3-hexylthiophen-2-yl)-1,3,2-dioxaborinane **4**[14] in the presence of $Pd(PPh_3)_4$ afforded a terthiophene-appended methyl ester **5** in 83% yield. The hydrolysis of **5** with KOH gave 2,5-di(3-hexylthiophen-2-yl)thiophene-3-carboxylic acid **6** in 96% yield, which was then used for the esterification of bis(6-hydroxyhexanyl)disulfide **7**[15] in the presence of 1-ethyl-3-(3-dimethylaminopropyl)carbodiimide hydrochloride (EDAC) and 4-dimethylaminopyridine (DMAP) to give **2** in 86% yield. Reagent **2** was characterized by ^1H NMR spectroscopy, FABMS, and elemental analyses after purification using flash column chromatography. The reagent was then used to prepare Au/terthiophene hybrid **1** as follows: a toluene solution of $AuCl_4^-(C_8H_{17})_4N^+$, which was generated in situ by reacting an aqueous solution of $HAuCl_4$ (1.70 mmol) with tetraoctylammonium bromide (3.81 mmol), was added to a toluene solution of **2** (0.95 mmol) in a two-neck flask. The resulting mixture was stirred for 30 min in an ice bath and was then treated with $NaBH_4$ (19.01 mmol). The solution became dark brown and was stirred for further 86 h in the dark to obtain **1**.

2.2. Characterization

The FTIR spectrum of the Au/terthiophene hybrid **1** showed vibration bands at 1711 and 1242 cm^{-1} that corresponded to an ester unit, indicating that the obtained gold nanoparticles were coated with ligands having terthiophene units. The particles were well-dispersed and dark brown after mixing with in chloroform. Fig. 1(red line) shows the UV/vis spectrum of **1** in $CHCl_3$; the absorbance at 325 nm is attributable to the π–π^* transition of terthiophene.[16] It is noteworthy that a surface plasmon resonance band near 520 nm was not clearly observed, suggesting the presence of gold nanoparticles having a core diameter of less than 2 nm.[17] We attempted to measure the average diameter of the gold core by high-angle annular dark-field scanning transmission electron microscopy (HAADF-STEM). Fig. 2a shows the TEM image of the Au/terthiophene hybrid **1**. Particle size distribution was taken from about 900 particles; the histogram shows that the average diameter of the gold nanoparticles was 1.9 nm with a standard deviation of 0.1 nm. It is worth noting that under the synthetic condition of $[AuCl_4^-]/[\mathbf{2}]=1.8$, monodispersed particles with small diameters could be obtained. Using Leff's model, the average number of gold atoms in the 1.9-nm-diameter core was found to be 220.[18] Powder X-ray diffraction (PXRD) patterns of the nanoparticles showed a broad peak at 38.3° corresponding to a *d*-spacing of 2.350 Å, which can be assigned to the {111} facet of a face-centered cubic lattice (Fig. 3a).[19] The rest of diffraction peaks

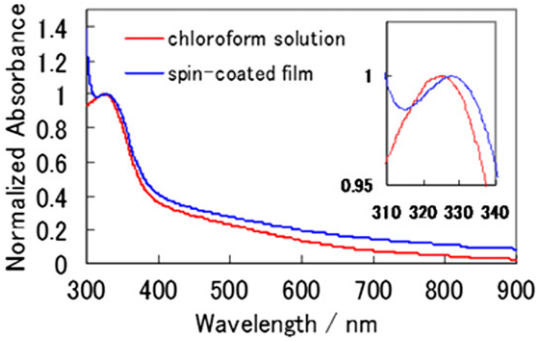

Fig. 1. UV/vis spectra of **1** in $CHCl_3$ (red line) and its spin-coated film (blue line). Inset: the magnified graph.

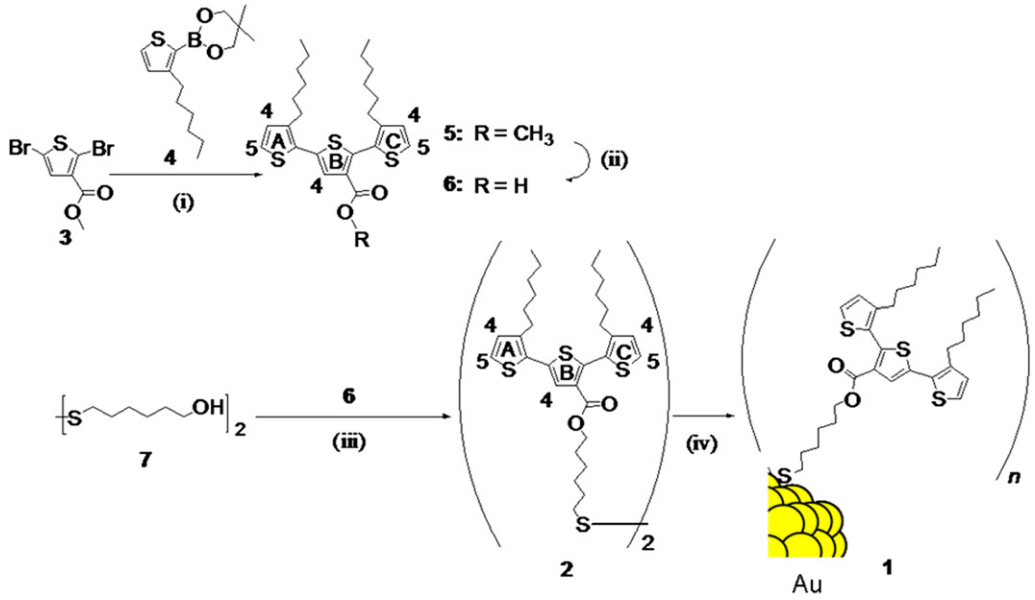

Scheme 1. Reagents and conditions: (i) $Pd(PPh_3)_4$, DME, 12 h, 80 °C, 83%; (ii) KOH, EtOH, 80 °C, 5.5 h, 96%; (iii) DMAP, EDAC, dry CH_2Cl_2, 63 h, 86%; (iv) $HAuCl_4 \cdot 4H_2O$ in the presence of tetraoctylammonium bromide and then $NaBH_4$.

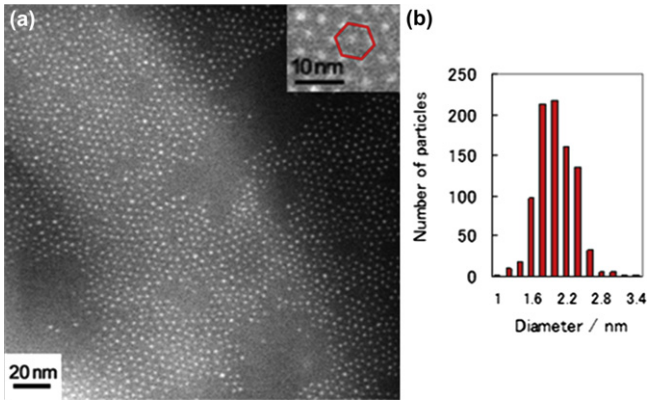

Fig. 2. (a) HAADF-STEM image of **1**. The inset shows magnified TEM image of (a). (b) Histogram of the Au core diameter measured from the TEM image.

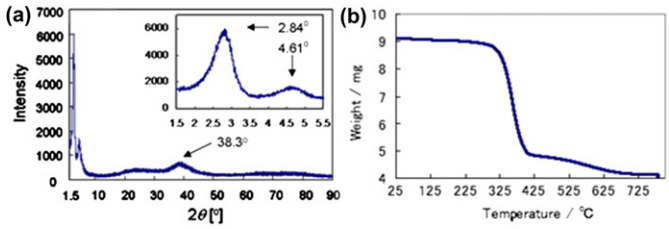

Fig. 3. (a) PXRD pattern (inset: PXRD pattern from 1.5° to 5.5°) and (b) thermogravigram of Au/terthiophene hybrid **1**. The graph (b) shows the loss of mass as a function of temperature. Conditions: nitrogen atmosphere and heating rate of 5 °C min^{-1} in the temperature range of 28–779 °C.

at 2θ=2.84° and 4.61° led to characteristic ratio of $1:1/\sqrt{3}$ for the *d*-spacings, suggesting that a hexagonal arrangement of the nanoparticles was formed. By performing elemental analysis, we determined the chemical composition of the nanoparticle surface; the percentage composition of C, H, and S was 34.11%, 4.03%, and 11.81%, respectively. In addition, the percentage composition of the residue was found to be 46.91%, which was consistent with that of Au. A thermogravimetric analysis indicated loss of mass from the coating layer after heating (54.5%) (Fig. 3b). From these results, we calculated the average ratio of Au atoms to the thiol-capping ligands to be 2.58. Thus, the number of ligand molecules attached to one Au particle was approximately 85.

2.3. Self-assembly of Au/terthiophene hybrid 1 and its film properties

A drop-cast film was prepared by using $CHCl_3$ solution of Au/terthiophene hybrid **1**. A TEM image of the film showed a hexagonal array of the nanoparticles (inset of Fig. 2a). The mean inter-particle spacing was estimated from the TEM image to be 2.3±0.1 nm, indicating that the face-to-face π–π interactions between the terthiophene parts occur in the hexagonally packed array, being shown (Fig. 4). Taken together, center-to-center distance between neighboring nanoparticles can be estimated to be 4.2 nm.

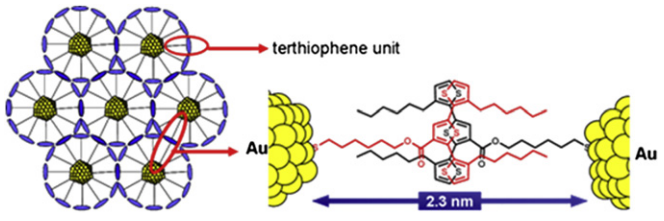

Fig. 4. Schematic of inter-ligand π–π interaction between neighboring **1**. Note: particles and terthiophene units are not drawn to scale.

To gain a better understanding of the film properties, we fabricated spin-coated films on a glass plate and measured the electric conductivity of the Au/terthiophene hybrid network in the films. A tapping-mode atomic force microscopy (AFM) of the film showed a smooth film with a height of ca. 164 nm (Fig. 5). The electric conductivity was measured using the two-probe technique by attaching fine gold wires to the spin-coated films with a carbon paste. The conductivity of the film without iodine doping was found to be 4.8×10^{-8} S cm^{-1}, and that of the iodine-doped film was estimated to be 9.1×10^{-6} S cm^{-1}, i.e., about 190 times that of the undoped film. The improved conductivity was ascribed to the π–π interactions among the terthiophene units in the network. However, we recognize that the conductivity of the film composed of **1** is lower than that of the terthiophenethiol-capped gold nanoparticles where the terthiophene units were directly linked to the gold,[20] as a result of the presence of an alkyl chain between the terthiophene and the gold core in **1**.[21] It should be noted that despite the low conductivity, the Au/terthiophene hybrid-containing film exhibited the property of electric conductivity.

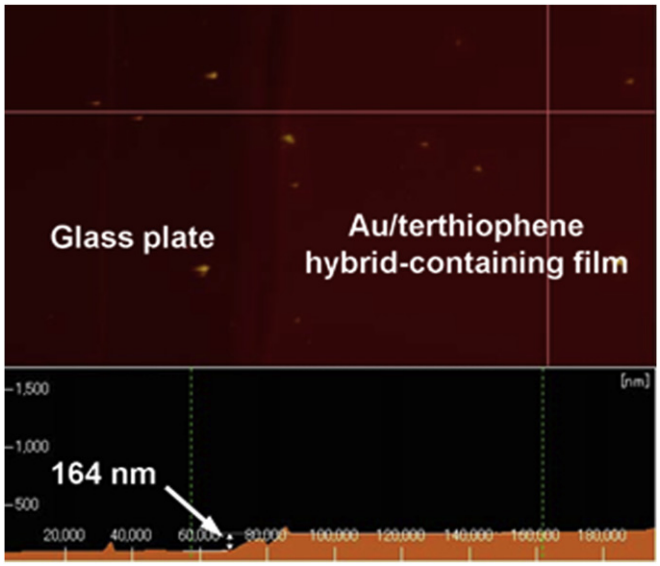

Fig. 5. AFM images of the Au/terthiophene hybrid-containing film.

The abovementioned results for electric conductivity in the films led us to carry out their structural analysis. The absorption band of the film was shifted to longer wavelength by 3 nm with respect to that measured in the $CHCl_3$ solution (Fig. 1 (blue line)). Grazing-incidence small-angle X-ray scattering (GISAXS) can be used for determining the internal morphologies of thin films.[22] A thin film of the Au/terthiophene hybrid was fabricated by spin-coating at 1000 rpm using the $CHCl_3$ solution, and the film was then deposited on a silicon wafer. GISAXS measurements of the film were carried out at α_i=0.17°, where α_i is the incident angle of the X-ray beam with respect to the film surface. Fig. 6 shows a 2D GISAXS pattern of the film. Several diffraction spots such as *R*1 and *R*2 were observed and these spots were attributed to the diffraction peaks of {10} and {11}, respectively. The relative scattering vector lengths of the in-plane diffraction peaks at 1.95 and 3.33 nm^{-1} were estimated to be 1 and $\sqrt{3}$, respectively, from the specular reflection position. The diffraction spots indicate the formation of a hexagonally arranged structure. The strong diffraction peak of *R*1 (q_y=1.95 nm^{-1}) afforded 3.22 nm as d_{10} value. Thus the center-to-center distance *a* between neighboring gold particles ($a = 2\times d_{10}/\sqrt{3}$) could be calculated to be 3.72 nm, which is almost consistent with the value deduced by TEM measurement when we take into the diameter of the gold core (1.9±0.1 nm) and

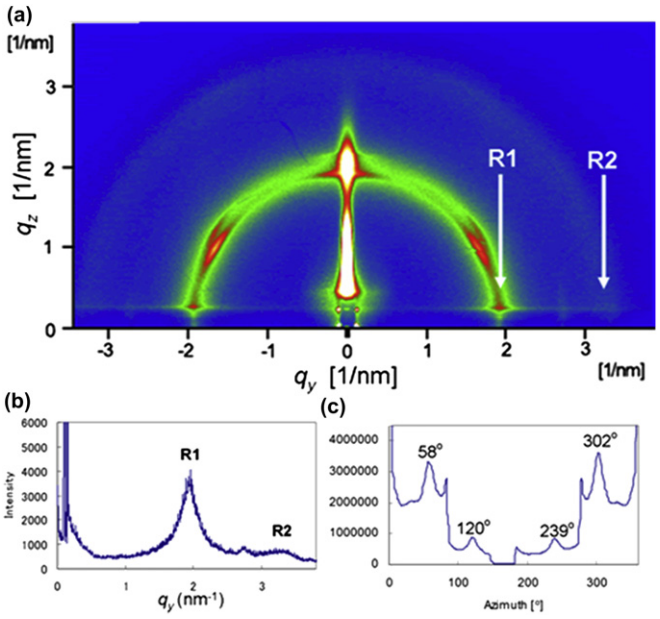

Fig. 6. (a) 2D GISAXS pattern measured at incident angle of 0.17° for Au/terthiophene hybrid-containing film. (b) In-plane intensity profile extracted at grazing exit angle of 0.17° from scattering pattern. (c) Azimuthal scan of the pattern.

the inter-particle spacing (2.3±0.1 nm) account. In addition, the 2D GISAXS pattern showed circular lines (Debye–Scherrer lines) along with a few diffraction spots (Fig. 6a). From an azimuthal scan of the pattern (Fig. 6c), we found that the intensity of these reflections exhibited a six-fold symmetry, suggesting that either a hexagonal close-packed or a face-centered cubic lattice of the nanoparticles, or both those lattices may be formed in the film. All these findings together indicate that three-dimensional arrays of the Au/terthiophene hybrids were macroscopically organized in these films, resulting in the formation of a π-stacked array of the terthiophenes that induced the electric conductivity in the films.

3. Conclusion

In this work, monodispersed gold nanoparticles **1** with π-conjugated terthiophenes at the surface were newly prepared by using the method proposed by Brust et al. In this method, $AuCl_4^-$ was reduced using $NaBH_4$ with bis(terthiophene)-derived disulfide **2**. GISAXS measurement of the spin-coated film indicated that macroscopically gold nanoparticle-templated alignment of terthiophenes enabled electric communication via inter-ligand face-to-face π–π interactions among the terthiophene units. Although modifications will be required to further optimize the conductivity, we believe that a better understanding of the factors that affect the three-dimensional organization of oligothiophenes will facilitate the development of new inorganic/organic hybrid systems.

4. Experimental section

4.1. Measurements

NMR spectra were taken a JEOL JNM-EX270 spectrometer. Chemical shifts (δ) are reported downfield from the initial standard Me_4Si. Fast atom bombardment (FAB) mass spectra were obtained on a JEOL JMS-700 spectrometer where *m*-nitrobenzyl alcohol was used as a matrix. High-angle annular dark-field scanning transmission electron microscopy (HAADF-STEM) was carried out using JEOL JEM-3200FS. The intensity data of powder X-ray diffraction (PXRD) was collected by Rigaku RINT-TTR III powder diffractometer. Infrared spectrum was taken on Jasco FT-IR-5300. Absorption spectra and thermogravimetric analysis (TGA) were obtained on Shimadzu UV-3100PC spectrophotometer and Shimadzu DTA-60H, respectively. Elemental analyses were obtained using Yanaco CHNCORDER MT-5 for assigning **2** and Yanaco CHN CORDER MT-6/J-SCIENCE LAB MICRO CORDER JM10/Dionex ICS-1500 Ion chromatography for assigning **1**, respectively. KEYENCE VN-8000 nanoscale hybrid microscope was used for recording AFM image. The electric conductivity was evaluated using KEITHLEY 6517A Electrometer. Grazing-incidence small-angle X-ray scattering (GISAXS) studies were performed with NANO VIEWER (Rigaku) equipped with Micro Max-007HF high intensity micro focus rotating anode X-ray generator (1.4 kW, Cu Kα).

4.2. Materials

Reagents used for the synthesis were commercially available and used as supplied. Methyl 2,5-dibromothiophene-3-carboxylate **3** was prepared from methyl thiophene-3-carboxylate via dibromination with Br_2. 5,5-Dimethyl-2-(3-hexylthiophen-2-yl)-1,3,2-dioxaborinane **4** was straightforwardly synthesized via bromination, bolyration, and boronate esterification with 2,2-dimethyl-1,3-propanediol. Bis(6-hydroxyhexanyl)disulfide **7** was obtained from oxidation reaction of 6-hydroxyhexanylthiol with iodine.

4.3. Synthesis

*4.3.1. Methyl 2,5-di(3-hexylthiophen-2-yl)thiophene-3-carboxylate (**5**).* Methyl 2,5-dibromothiophene-3-carboxylate **3** (1.08 g, 3.61 mmol), 5,5-dimethyl-2-(3-hexylthiophen-2-yl)-1,3,2-dioxaborinane **4** (3.99 g, 14.2 mmol), and 1 M Na_2CO_3 (15 mL) were added to 1,2-dimethoxyethane (20 mL). $Pd(PPh_3)_4$ (260 mg, 0.225 mmol) was then added to the solution and the resulting solution was stirred at 80 °C for 12 h under an N_2 condition. After extraction with CH_2Cl_2 (90 mL), the organic phase was dried with Na_2SO_4 and evaporated in vacuo. The residue was chromatographed on silica gel (Wakogel C-300, AcOEt (3% (v/v))) in hexane as an eluent. In this way, 1.43 g of **5** was obtained as a yellow oil in 83% yield. ^{1}H NMR ($CDCl_3$, 270 MHz) δ 7.50 (1H, s, Th^{B4}–H), 7.34 (1H, d, J=5.1 Hz, Th^{C5}–H), 7.21 (1H, d, J=5.1 Hz, Th^{A5}–H), 6.96 (1H, d, J=5.4 Hz, Th^{C4}–H), 6.94 (1H, d, J=5.1 Hz, Th^{A4}–H), 3.73 (3H, s, $-OCH_3$), 2.76 (2H, t, J=7.7 Hz, Th^{C}–CH_2), 2.53 (2H, t, J=7.7 Hz, Th^{A}–CH_2), 1.69–1.49 (4H, m, Th–CH_2CH_2), 1.39–1.21 (12H, m, Th–$CH_2CH_2(CH_2)_3CH_3$), 0.87 (3H, t, J=6.9 Hz Th^{C}–$(CH_2)_5CH_3$), 0.84 (3H, t, J=6.8 Hz, Th^{A}–$(CH_2)_5CH_3$); FABMS m/z 474 [M^+]; IR (CH_2Cl_2 solution): selected absorptions; 1723, 1248 cm^{-1}.

*4.3.2. 2,5-Di(3-hexylthiophen-2-yl)thiophene-3-carboxylic acid (**6**).* Methyl 2,5-di(3-hexylthiophen-2-yl)thiophene-3-carboxylate **5** (755 mg, 1.59 mmol) was added to 0.5 M KOH ethanol solution (30 mL). The resulting solution was stirred under reflux for 5.5 h, cooled to room temperature, acidified (pH 2) by adding 1 M HCl aqueous solution, and then extracted with CH_2Cl_2 (150 mL). The organic phase was dried with Na_2SO_4 and evaporated in vacuo. In this way, 0.706 g of 6 was obtained as a brown oil in 96% yield. ^{1}H NMR ($CDCl_3$, 270 MHz) δ 7.53 (1H, s, Th^{B4}–H), 7.35 (1H, d, J=5.1 Hz, Th^{C5}–H), 7.21 (1H, d, J=5.1 Hz, Th^{A5}–H), 6.97 (1H, d, J=5.1 Hz, Th^{C4}–H), 6.94 (1H, d, J=5.1 Hz, Th^{A4}–H), 2.76 (2H, t, J=7.7 Hz, Th^{C}–CH_2), 2.54 (2H, t, J=7.7 Hz, Th^{A}–CH_2), 1.69–1.50 (4H, m, Th–CH_2CH_2), 1.39–1.22 (12H, m, Th–$CH_2CH_2(CH_2)_3CH_3$), 0.90–0.80 (6H, m, $-CH_3$); FABMS m/z 460 [M^+]; IR (CH_2Cl_2 solution): selected absorptions; 1688, 1265 cm^{-1}.

*4.3.3. Bis[2,5-di(3-hexylthiophen-2-yl)thiophene-3-carboxyloxyhexanyl]disulfide (**2**).* Bis(6-hydroxyhexanyl)disulfide (52.6 mg, 0.197 mmol), 2,5-di(3-*n*-hexylthiophen-2-yl)thiophene-3-carboxylic

acid (200 mg, 0.434 mmol), 4-(dimethylamino)pyridine (5.2 mg, 0.0426 mmol), and 1-ethyl-3-(3-dimethylaminopropyl)carbodiimide hydrochloride (83.3 mg, 0.435 mmol) were dissolved in dry CH_2Cl_2 (6 mL) in ice bath. The resulting mixture was stirred at 30 °C for 38 h and then partitioned with distilled water (100 mL). The organic phase was dried with Na_2SO_4 and evaporated in vacuo. The residue was chromatographed on silica gel (Wakogel C-300, hexane/$CHCl_3$ as an eluent). In this way, 0.197 g of **2** was obtained as a yellow oil in 86% yield. ^{1}H NMR ($CDCl_3$, 270 MHz) δ 7.50 (2H, s, Th^{B4}–H), 7.33 (2H, d, J=5.1 Hz, Th^{C5}–H), 7.21 (2H, d, J=5.1 Hz, Th^{A5}–H), 6.95 (2H, d, J=5.1 Hz, Th^{C4}–H), 6.94 (2H,d, J=5.4 Hz, Th^{A4}–H), 4.11 (4H, t, J=6.3 Hz, $-OCH_2$), 2.76 (4H, t, J=7.7 Hz, Th^{C}–CH_2), 2.66 (4H, t, J=7.3 Hz, $-SCH_2$), 2.52 (4H, t, J=7.7 Hz, Th^{A}–CH_2), 1.70–1.46 (8H, m, Th–CH_2CH_2), 1.39–1.15 (40H, m, Th–$CH_2CH_2(CH_2)_3CH_3$, Th–$^{-}COOCH_2(CH_2)_4CH_2S$), 0.91–0.81 (12H, m, $-CH_3$); FABMS m/z 1150[M^+]; IR (CH_2Cl_2 solution): selected absorptions; 1707, 1267 cm^{-1}. Anal. Calcd for $C_{62}H_{86}O_4S_8$: C, 64.65; H, 7.53. Found: C, 64.19; H, 7.55%.

*4.3.4. Preparation of Au/terthiophene (**1**).* $HAuCl_4 \cdot 4H_2O$ (701 mg, 1.70 mmol) and tetraoctylammonium bromide (2.09 g, 3.81 mmol) were dissolved in distilled water (100 mL) and toluene (220 mL), respectively. The biphasic mixture was vigorously stirred until the tetrachloroaurate was entirely transferred into the organic phase. The organic phase was added to toluene solution (20 mL) of **2** (1.09 g, 0.950 mmol). The resulting solution was vigorously stirred for 30 min in ice bath. $NaBH_4$ (719 mg, 19.0 mmol), being dissolved in distilled water (100 mL), was added to the solution. Subsequently, the solution was stirred at room temperature for 86 h under a dark condition. The organic phase was separated off and evaporated concentrated in vacuo. The obtained nanoparticles were purified by toluene/ethanol reprecipitation process wherein the nanoparticles were centrifuged (2000 rpm, 20 min) and then collected. The procedure was repeated in three times. In this way, 741 mg of **1** was obtained as a dark brown viscous solid. IR (KBr disc): selected absorptions; 1711, 1242 cm^{-1}; Elemental analysis: C, 34.11; H. 4.03; S, 11.81; Au, 46.91%.

4.4. Preparation of the TEM grid

For the observation, a carbon-supported copper grid (elastic carbon substrate on STEM100Cu grids, Okenshoji Co., Ltd) was used. A toluene solution containing **1** (0.1 mg mL^{-1}) was dropped onto the grid, being dried naturally for one day before the TEM observation.

4.5. Procedure of the electric conductivity measurement

Au/terthiophene **1** (13.04 mg) was dissolved in $CHCl_3$ (0.5 mL), the resulting solution being spin-coated on glass plate with 1000 rpm. The thickness was estimated by AFM to be 164 nm. Electric conductivity was measured by the two-probe techniques using fine gold wires attached to spin-coated films with carbon paste.

4.6. GISAXS measurement of the film

A $CHCl_3$ solution of Au/terthiophene hybrid **1** (26.08 g L^{-1}) was dropped onto a silicon wafer. The spin-coated film was prepared at a constant speed of 1000 rpm and dried in the air. X-ray was incident on the hybrid film under a fixed angle of 0.17°. The data were collected during 24 h using an X-ray wavelength (λ) of 1.5418 Å on a two-dimensional position sensitive vacuum chamber detector at 607 mm from the sample. Scattering patterns were collected on an imaging plate (FUJIFILM BAS-SR) and detected with an imaging plate detector (Rigaku RAXIS-DS3C). Obtained peak intensities were reported against scattering vector q, which is equal to $4\pi(\sin\theta)/\lambda$ (2θ is the diffusion angle). The recording plate, indicated by the q_y- and q_z-axes, corresponds to a two-dimensional detector. d-Spacings are calculated from scattering vector q via following equation; $d=2\pi/q$.

Supplementary data

Supplementary data associated with this article can be found in the online version at doi:10.1016/j.tet.2011.10.032.

References and notes

1. (a) Tour, J. M. *Acc. Chem. Res.* **2000**, *33*, 791–804; (b) Bunz, U. H. *Chem. Rev.* **2000**, *100*, 1605–1644; (c) Mishra, A.; Ma, C.-Q.; Bäuerle, P. *Chem. Rev.* **2009**, *109*, 1141–1276; (d) Heeger, A. J. *Chem. Soc. Rev.* **2010**, *39*, 2354–2371.
2. (a) Kline, R. J.; McGehee, M. D. *Polym. Rev.* **2006**, *46*, 27–45; (b) Ong, B. S.; Wu, Y.; Li, Y.; Liu, P.; Pan, H. *Chem.—Eur. J.* **2008**, *14*, 4766–4778.
3. Current reviews, see: (a) Tang, W.; Hai, J.; Dai, Y.; Huang, Z.; Lu, B.; Yuan, F.; Tang, J.; Zhang, F. *Sol. Energy Mater. Sol. Cells* **2010**, *94*, 1963–1979; (b) Brabec, C. J.; Heeney, M.; McCulloch, I.; Nelson, J. *Chem. Soc. Rev.* **2011**, *40*, 1185–1199; (c) Ruderer, M. A.; Müller-Buschbaum, P. *Soft Matter* **2011**, *7*, 5482–5493.
4. (a) Tang, B. Z. *Macromol. Chem. Phys.* **2009**, *210*, 900–902; (b) Li, C.; Bo, Z. *Polymer* **2010**, *51*, 4273–4294.
5. (a) Hoeben, F. J. M.; Jonkheijm, P.; Meijer, E. W.; Schenning, A. P. H. J. *Chem. Rev.* **2005**, *105*, 1491–1546; (b) Thomas, S. W., III; Joly, G. D.; Swager, T. M. *Chem. Rev.* **2007**, *107*, 1339–1386.
6. (a) *Electric Materials: The Oligomer Approach*; Müllen, K., Wegner, G., Eds.; VCH: Weinheim, 1998; (b) Leclère, Ph.; Surin, M.; Viville, P.; Lazzaroni, R.; Kilbinger, A. F. M.; Henze, O.; Feast, W. J.; Cavakllini, M.; Biscarini, F.; Schenning, A. P. H. J.; Meijer, E. W. *Chem. Mater.* **2004**, *16*, 4452–4466.
7. Shaw, C. P.; Fernig, D. G.; Lévy, R. *J. Mater. Chem.* **2011**, *21*, 12181–12187.
8. Descalzo, A. B.; Martínez-Máñez, R.; Sancenón, F.; Hoffmann, K.; Rurack, K. *Angew. Chem., Int. Ed.* **2006**, *45*, 5924–5948.
9. van Herrikhuyzen, J.; George, S. J.; Vos, M. R. J.; Sommerdijk, N. A. J. M.; Ajayaghosh, A.; Meskers, S. C. J.; Schenning, P. H. J. *Angew. Chem., Int. Ed.* **2007**, *46*, 1825–1828.
10. (a) Sih, B. C.; Wolf, M. O. *Chem. Commun.* **2005**, 3375–3384; (b) Prakash, A.; Ouyang, J.; Lin, J.-L.; Yang, Y. *J. Appl. Phys.* **2006**, *100*, 054309; (c) Zotti, G.; Vercelli, B.; Berlin, A. *Acc. Chem. Res.* **2008**, *41*, 1098–1109; (d) Park, D. H.; Kim, M. S.; Joo, J. *Chem. Soc. Rev.* **2010**, *39*, 2439–2452; (e) Stavytska-Barba, M.; Kelley, A. M. *J. Phys. Chem. C* **2010**, *114*, 6822–6830.
11. Minami, T.; Nishiyabu, R.; Iyoda, M.; Kubo, Y. *Chem. Commun.* **2010**, 8603–8605.
12. Brust, M.; Walker, M.; Bethell, D.; Schiffrin, D. J.; Whyman, R. *J. Chem. Soc., Chem. Commun.* **1994**, 801–802.
13. Gambhir, S.; Wagner, K.; Officer, D. L. *Synth. Met.* **2005**, *154*, 117–120.
14. Janzen, D. E.; Burand, M. W.; Ewbank, P. C.; Pappenfus, T. M.; Higuchi, H.; da Silva Filho, D. A.; Young, V. G.; Brédas, J.-L.; Mann, K. R. *J. Am. Chem. Soc.* **2004**, *126*, 15295–15308.
15. Wang, X.; Ramström, O.; Yan, M. *Anal. Chem.* **2010**, *82*, 9082–9089.
16. It is known that 2,5-di(3-octylthiophen-2-yl)thiophene has λ_{max} of 337 nm in CH_2Cl_2, see: Liu, Y.; Zhou, J.; Wan, X.; Chen, Y. *Tetrahedron* **2009**, *65*, 5209–5215.
17. Daniel, M.-C.; Astruc, D. *Chem. Rev.* **2004**, *104*, 293–346.
18. Leff, D. V.; Ohara, P. C.; Heath, J. R.; Gelbart, W. M. *J. Phys. Chem.* **1995**, *99*, 7036–7041.
19. Standard value of d-spacing for {111} facet is 2.355 based on JCPDS.
20. Zotti, G.; Vercelli, B.; Berlin, A. *Chem. Mater.* **2008**, *20*, 397–412.
21. Ahn, H.; Chandekar, A.; Kang, B.; Sung, C.; Whitten, J. E. *Chem. Mater.* **2004**, *16*, 3274–3278.
22. (a) Lee, B.; Park, Y.-H.; Hwang, Y.-T.; Oh, W.; Yoon, J.; Ree, M. *Nat. Mater.* **2005**, *4*, 147–150; (b) Lee, B.; Park, I.; Yoon, J.; Park, S.; Kim, J.; Kim, K.-W.; Chang, T.; Ree, M. *Macromolecules* **2005**, *38*, 4311–4323.